

# Adaptive Variable-Current Wireless Charging for Electric Vehicles with Higher Power Transfer Capability

Zhichao Hua<sup>1</sup>, K. T. Chau<sup>1</sup>, Tengbo Yang<sup>1</sup>, Hongliang Pang<sup>1</sup>, and Qi Zhu<sup>2</sup>

<sup>1</sup>Department of Electrical and Electronic Engineering, The University of Hong Kong, Hong Kong, China

(Email: ktchau@eee.hku.hk)

<sup>2</sup>Beijing Xiaomi Mobile Software Co., Ltd, Beijing, China

---

## Executive Summary

This paper proposes an adaptive variable-current wireless charging system for electric vehicles (EVs) using self-excited oscillation (SEO), in which the operating frequency can change adaptively and variable-current charging with two-stage constant-current (CC) phases is adopted. The proposed adaptive SEO wireless charging system exhibits higher power transfer capability when the battery resistance is smaller than a certain value compared with the traditional forced oscillating (FO) wireless charging system that operates on the fixed resonant frequency. The variable-current charging contributes to faster charging for the EV battery. The simulation results have verified the feasibility of the proposed adaptive variable-current wireless charging system.

*Keywords: Adaptive variable current, wireless charging, higher power transfer capability, electric vehicles*

---

## 1 Introduction

As wireless power transfer (WPT) system shows the key advantages of low maintenance, flexibility, convenience and electrical isolation [1]–[4], it can be applied to many areas, such as wireless heating [5]–[8], wireless motor [9]–[12], wireless lighting [13]–[16] and wireless charging for implant applications [17]–[20]. In recent years, electric vehicles (EVs) are becoming popular and are replacing gasoline vehicles. The charging technologies for EV batteries [21]–[24] are of great significance, and it is the most possible way to become another mainstream charging scheme apart from the wired charging station. The possible charging scenarios include static wireless charging [25]–[27] in a wireless charging station or dynamic wireless charging [28]–[31] on a road where the EVs keep moving.

No matter which scenario, the charging speed is one of the most important functions that draw consumers' attention. Normally, the voltage level of the microgrid supplying the wireless charging station is fixed. Under this restriction, it is desirable to improve the power transfer capability of the wireless charging system. One of the ways to increase the transfer power capability is to improve the voltage level of the DC microgrid that supplies a wireless charging system, but an additional boost converter is required. Also, if the voltage level

is too high, the voltage class of the MOSFETs will be higher for wireless charging for EV batteries. For a traditional wireless charging system with a series-series (SS) topology and fixed operating frequency, the maximum charging current is also fixed.

To improve the transfer power capability, instead of increasing the input DC voltage, the compensation scheme can be adopted, but this will require more compensation components and increase the complexity of the system [32]-[33]. The mainstream charging scheme is an initial constant-current (CC) charging phase and a subsequent constant-voltage (CV) charging phase. Most power is charged in the CC phase. It has been also researched that variable-current charging with multi-stage CC phases for batteries can promote fast charging [34], avoid severe temperature rise and extend cycle life [35]. Thus, variable-current charging should attract more attention.

Also, to make the charging current and voltage follows the reference values, a proper modulation scheme is needed. There are many modulation schemes to regulate the output of a wireless charging system, such as burst firing control (BFC) [36]-[38], phase shift control (PSC) [39]-[42] and pulse frequency modulation (PFM) [43]-[46]. The PSC has the disadvantage of the hard-switching problem, which will reduce the system efficiency. The BFC can achieve ZVS and are free of hard-switching loss, but it will cause nonnegligible output fluctuations. PFM has the merit of fewer fluctuations and realizing ZVS easily.

Also, the traditional WPT systems normally operate on the resonant frequency and the operating frequency is fixed. The WPT systems based on self-excited oscillation (SEO) [47]-[50] can make the system operate on the splitting frequency. Compared to the traditional WPT system, it can output higher power in the splitting region. This advantage can be utilized in wireless charging for electric vehicles as fast charging is desired by consumers.

This paper proposes an adaptive variable-current wireless charging system using SEO so that the operating frequency can change adaptively. When the battery resistance is smaller than a certain value, the system is in the splitting region, and the proposed adaptive SEO wireless charging system exhibits higher power transfer capability compared with the traditional forced oscillating (FO) wireless charging system that operates on the fixed resonant frequency. Also, a variable-current charging scheme with two-stage CC phases is adopted. Autonomous pulse frequency modulation (APFM) and feedback control for the adaptive wireless charging system is adopted to achieve variable-current and CV charging. The simulation results have verified the feasibility of the proposed adaptive variable-current wireless charging system.

## 2 System Configuration and Analysis

### 2.1 System Topology

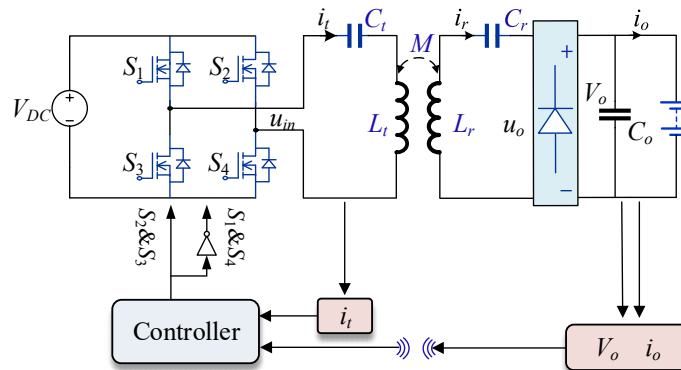


Figure 1: Proposed wireless charging system using PFM.

The proposed wireless charging system for EVs is shown in Figure 1, and the SS topology is adopted.  $L_t$  and  $L_r$  are the transmitter coil inductance and receiver coil inductance.  $C_t$  and  $C_r$  are the compensated capacitance of the transmitter side and receiver side.  $M$  is the mutual inductance.  $V_{DC}$  is the DC source voltage.  $V_o$  is the battery terminal voltage.  $I_o$  is the battery charging current.  $I_t$  and  $I_r$  are the transmitter current and receiver current, respectively. The transmitter current is sensed and provided to the controller. The controller will generate the driving signal that is dependent on the transmitter current. The transmitter current can help the system to operate on the SEO. Also, battery voltage and current are sensed to help realize the feedback control.

The adaptive wireless charging system operates as SEO [47-50] instead of the traditional FO that operates on the fixed resonant frequency. When the WPT system operates as FO, the operating frequency is fixed and normally set to be the resonant frequency. When the inverter output is the 50%-duty-ratio waveform, the output power is:

$$P_{out} = \frac{8V_{DC}^2}{\pi^2} \frac{R_o}{\left( \omega_0 k L_r \sqrt{L_t / L_r} + \frac{R_1 (R_2 + R_o)}{\omega_0 k L_r} \sqrt{L_r / L_t} \right)^2} \quad (1)$$

Where  $\omega_0$  is the resonant frequency of the WPT system and  $\omega_0 = \sqrt{1/(L_t C_t)} = \sqrt{1/(L_r C_r)}$ .

When adopting the proposed adaptive wireless charging system, the system operating frequency is not fixed to be resonant frequency. When  $k \geq k_c = (R_2 + R_o)/(\omega_0 L_2)$ , the system is in the splitting region, and the output power is:

$$P_{out} = \frac{8V_{DC}^2}{\pi^2} \frac{R_o}{\left( R_t \sqrt{L_r / L_t} + (R_r + R_o) \sqrt{L_t / L_r} \right)^2} \quad (2)$$

When  $k < k_c = (R_2 + R_o)/(\omega_0 L_2)$ , the system is not in the splitting region, the output power is the same as that of the FO-WPT system.

By comparing (1) and (2), it can be concluded that the output power based on SEO is larger than that based on FO when the wireless charging system is in the splitting region. For wireless charging for EV batteries, most power is transmitted through CC phase. The charging current is normally large and therefore the internal resistance is small. It is easy to achieve  $k \geq k_c = (R_2 + R_o)/(\omega_0 L_2)$ , thus making the system easy to be in the splitting region. It is more beneficial to use adaptive wireless charging schemes, which means that the operating frequency will be the splitting frequency adaptively.

## 2.2 Adaptive Variable-Current Wireless Charging

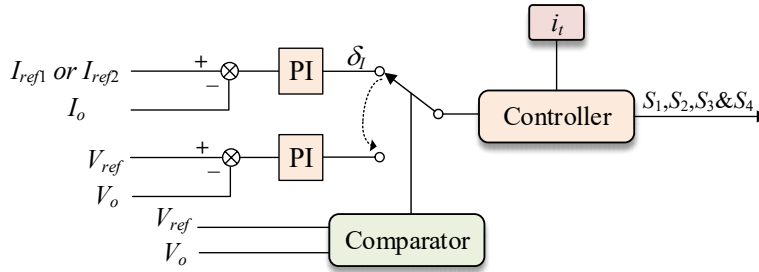


Figure 2: Control loop of proposed system.

One way for faster charging is to make the inverter output voltage to be 50%-duty-ratio voltage waveform and the system is based on SEO. However, the charging current will keep changing as the battery internal resistance changes, and it is not the usual case. Constant current charging is still desired. When adopting one-stage constant current charging, the charging current is limited by the voltage of the battery when the internal

resistance of the battery is constant and known, which will limit the battery charging speed. Multiple-stage CC charging will increase the charging power.

The variable-current charging scheme with two-stage CC phases is adopted for battery charging, followed by CV charging phase. Still, the transferred power can be larger than the traditional FO wireless charging system. As shown in Figure 2, the transmitter current is sensed to help the system operate on the SEO. Also, FPM is incorporated to this SEO wireless charging system and thus it is termed autonomous pulse frequency modulation (APFM). It means that the operating frequency of the APFM will change autonomously according to the system parameters. The current feedback loop and the voltage feedback loop are adopted to help change the duty ratio of the APFM. When the system is in the CC phases, the charging current is controlled to be equal to the reference currents by regulating the duty ratio of APFM through a proportional-integral (PI) controller. The battery internal resistance will increase during the charging process. In the first CC phase, the charging current is controlled to be  $I_{ref1}$  and keep constant until the battery voltage reaches the maximum value. Then the second CC phase begins, and the charging current is controlled to be  $I_{ref2}$  and keep constant.  $I_{ref2}$  is smaller than  $I_{ref1}$  so that the battery voltage will not exceed the maximum voltage value. When the battery voltage reaches the maximum value again, the system enters into the CV phase, and the charging voltage is controlled to be equal to the desired voltage  $V_{ref}$  by regulating the duty ratio of APFM.

Also, to make the system exhibit higher power transfer capability, it is normally designed that the system is in the splitting region when the system is in two CC phases. This is easy to achieve as the battery internal resistance is normally small in CC phases and  $k \geq k_c = (R_2 + R_o) / (\omega_0 L_2)$  can be easily achieved.

When the system is in the splitting region, the output power when adopting APFM is:

$$P_{APFM} = \frac{8D_1^2 V_{DC}^2}{\pi^2} \frac{R_o}{\left( R_t \sqrt{L_r / L_t} + (R_r + R_o) \sqrt{L_t / L_r} \right)^2} \quad (3)$$

where  $D_1$  is the duty ratio of APFM

The output power when adopting the traditional PFM scheme is:

$$P_{PFM} = \frac{8D_2^2 V_{DC}^2}{\pi^2} \frac{R_o}{\left( \omega_0 k L_r \sqrt{L_t / L_r} + \frac{R_1 (R_2 + R_o)}{\omega_0 k L_r} \sqrt{L_r / L_t} \right)^2} \quad (4)$$

where  $D_2$  is the duty ratio of traditional PFM.

### 2.3 Charging Power Analysis

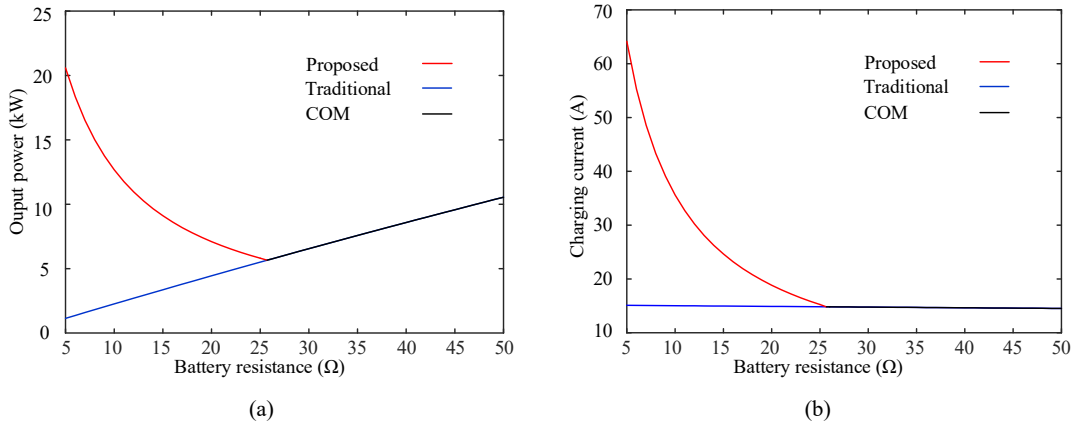


Figure 3: Theoretical maximum charging power and maximum charging current against battery resistance when  $V_{DC} = 400$  V. (a) Charging power. (b) Charging current.

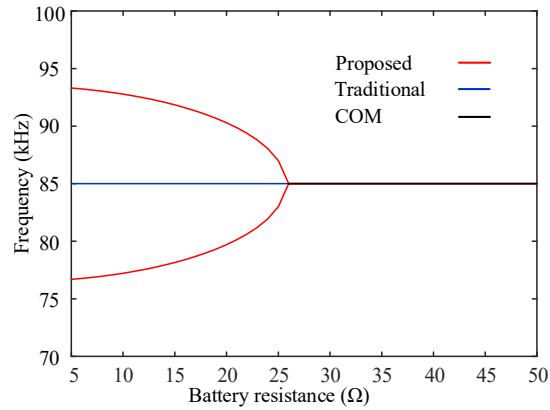


Figure 4: Theoretical operating frequency against battery resistance.

The load resistance ranging from  $5 \Omega$  to  $50 \Omega$  is considered. The transmitter and receiver coil inductance are  $200 \mu\text{H}$  and both of their internal resistances are  $0.5 \Omega$ . The mutual inductance is  $40 \mu\text{H}$ . The primary and secondary compensated capacitances are resonant with the transmitter and receiver coil inductances, and the resonant frequency is  $85 \text{ kHz}$ . The DC voltage  $V_{DC}$  is  $400\text{V}$ . The maximum charging power and maximum charging current are plotted in Figure 3(a) and Figure 3(b) using the traditional FO wireless charging system and the proposed adaptive SEO wireless charging system. The maximum charging power and charging current are achieved when the AC voltage of the inverter on the transmitter side is 50%-duty-ratio square waveform. It can be observed, the maximum charging power and charging current of the system that adopts SEO is larger than the system that adopts FO when the battery resistance is smaller than a certain value (about  $25 \Omega$ ).

The corresponding operating frequencies of these two schemes are plotted in Figure 4. It can be observed that the operating frequency of the proposed adaptive SEO wireless charging system is not fixed and is related to the battery resistance, while the operating frequency of the traditional FO wireless charging system is fixed and equal to the resonant frequency  $85 \text{ kHz}$ . Also, as shown in Figure 3 and Figure 4, when the battery resistance is larger than a certain value (about  $25 \Omega$ ), the proposed adaptive wireless charging system is equivalent to the traditional FO wireless charging system as they are plotted in common (COM) using the black line.

### 3 System Realization Consideration

#### 3.1 Signal Processing Circuit

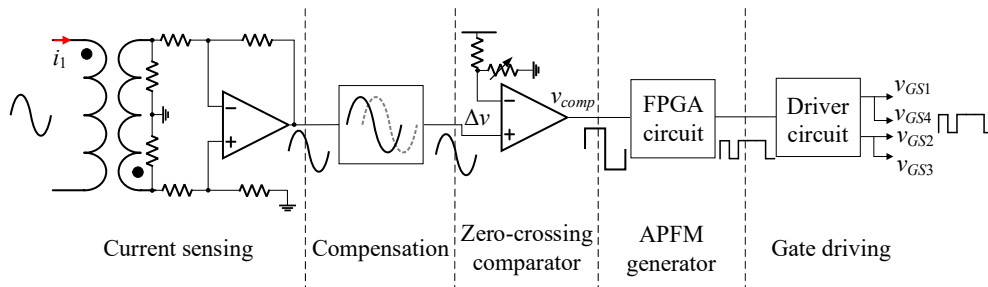


Figure 5: Signal processing circuit.

Figure 5 shows the signal processing circuit of the proposed system. To achieve the SEO wireless charging system, the operation of the inverter is related to the zero-crossing point of the transmitter current. The primary current is first sensed through a transformer. Then through a compensation circuit and a zero-crossing comparator, the square wave can be obtained, and it can be processed by the field-programmable gate array (FPGA) board. It should be noted this square wave is related to the transmitter current. Through FPGA, the APFM signal can be generated. Finally, the inverted can be derived by sending the APFM signal to the driving circuit.

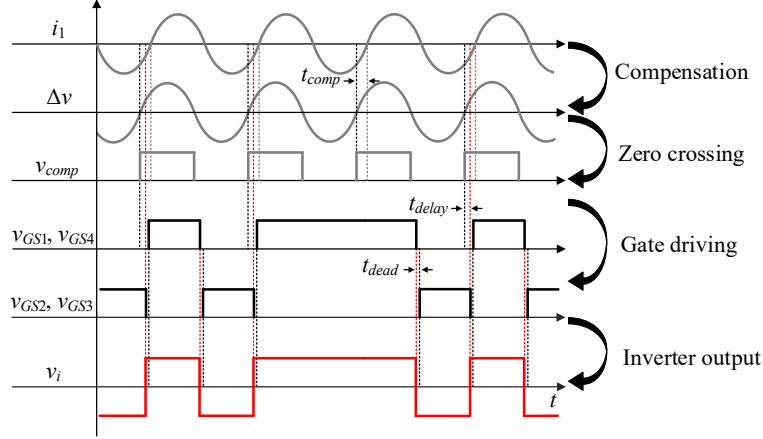


Figure 6: Waveforms for APFM generation.

The detailed signal waveforms of the signal processing are shown in Figure 6.  $V_{comp}$  is the output signal of the zero-crossing comparator. As the impact of the compensation circuit, the rising and falling edges will lead zero-crossing points of the transmitter current by a time  $t_{comp}$ . This leading time  $T_{comp}$  is designed to compensate the delay of the driving circuit.  $T_{comp}$  should be larger than the delay time  $t_{delay}$  of the driving circuit. By sending  $v_{comp}$  to the FPGA and programming FPGA, the FPGA board can generate the APFM signal. Through the driving circuit, the driving signal also leads the transmitter current  $t_{comp}-t_{delay}$ . Thus, zero-voltage switching can be achieved. Also, the dead time  $t_{dead}$  should be configured in the driving signals to avoid shoot-through problems.

### 3.2 Start-Up Consideration

For an SEO wireless charging system, the operation of the inverter is related to the transmitter current state. However, there is no current when the system is not operating. The system will be malfunctioning during start-up.

Therefore, the transmitter current should be produced first. This can be achieved by making the system operate on the resonant frequency. The operating frequency is fixed and not related to the transmitter current, which means that the system is a FO wireless charging system. After the transmitter current is produced, the system can then be switched to the SEO wireless charging system. Both the fixed frequency driving signal and the APFM signal can be generated by programming FPGA. Through the driving circuit, the inverter can operate as required.

## 4 Verifications and Discussions

To verify the proposed adaptive variable-current wireless charging system for EVs, the circuit simulation is conducted. The designed parameters are shown in Table 1. The battery voltage in the CV phase is 320V in this simulation. Figure 7 demonstrates two cases of transmitter voltage and current. When the load resistance is 10  $\Omega$ , the duty ratio of the APFM is 15/17. When the load resistance is 20  $\Omega$ , the duty ratio of APFM is 7/9. The equivalent fundamental transmitter voltage can be changed by regulating the duty ratio of APFM, thus

regulating the charging voltage and current. Also, when the load resistance is  $10 \Omega$ , the simulated operating frequency is measured as 76.9 kHz, when the load resistance is  $20 \Omega$ , the simulated operating frequency is measured as 82.6 kHz, which means that the system is operating on the splitting frequency, which is consistent with Figure 4.

Figure 8 shows the charging current and voltage when the battery resistance changes. The reference current in CC phase I is 32A and the reference current in CC phase II is 16 A. The reference voltage in the CV phase is 320V. The simulation results show that the charging current of CC phase I can reach the reference current 32A and the charging current of CC phase II can reach reference current 16 A, which are both larger than the theoretical maximum charging current in Figure 2(b) (about 14A) when using the traditional FO wireless charging system. In the CV phase, the terminal voltage of the battery can maintain 320V. It should also be noted that the actual EV battery voltage is smoother during the charging process.

The simulation results prove that the proposed adaptive SEO wireless charging system presents higher power transfer capability than the traditional FO wireless charging system, contributing to faster wireless charging for EV batteries.

Table 1: Design specifications and parameters

Items	Value
DC power grid voltage ( $V_{DC}$ )	400 V
Transmitter coil inductance ( $L_t$ )	200 $\mu$ H
Transmitter series compensated capacitance ( $C_t$ )	17.53 nF
Transmitter coil internal resistance ( $R_t$ )	0.5 $\Omega$
Receiver coil inductance ( $L_r$ )	200 $\mu$ H
Receiver series compensated capacitance ( $C_r$ )	17.53nF
Receiver coil internal resistance ( $R_r$ )	0.5 $\Omega$
Mutual inductances ( $M$ )	40 $\mu$ H
Operating frequency ( $f$ )	85 kHz
Output capacitance ( $C_o$ )	40 $\mu$ F

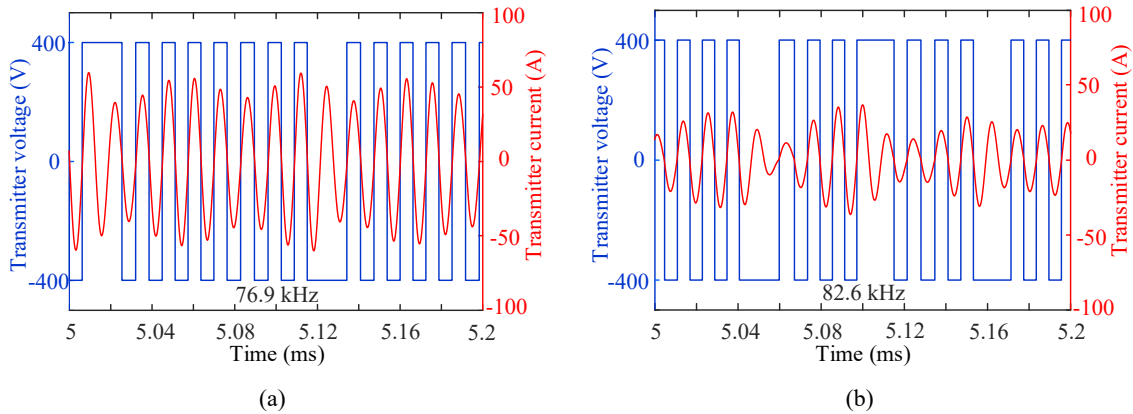


Figure 7: Simulation results. (a) Example of transmitter voltage and current under CC charging mode when the load resistance is  $10 \Omega$ . (b) Example of output voltage and current under CV charging mode when the load resistance is  $20 \Omega$ .

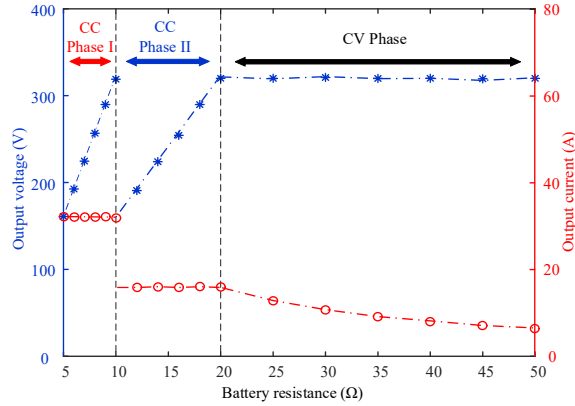


Figure 8: Output voltage and current against load resistance.

## 5 Conclusions

This paper has proposed an adaptive variable-current wireless charging system for electric vehicles. Two-stage CC phases are adopted. The WPT system operates based on SEO. The operating frequency of the system will change adaptively. When the system is in the splitting region, the system will operate on the splitting frequency and the output power is larger than that of the traditional FO wireless charging system. Feedback control and APFM are adopted to help the system achieve CC charging and CV charging. The realization method and the signal details are also suggested. The simulation results have validated the feasibility of the proposed adaptive variable-current wireless charging system.

## Acknowledgments

The work described in this paper was fully supported by a grant from the Research Grants Council of the Hong Kong Special Administrative Region, China (Project No. T23-701/20-R).

## References

- [1] W. Liu, K. T. Chau, C.H.T. Lee, C. Jiang, W. Han, and W.H. Lam, "Multi-frequency multi-power one-to-many wireless power transfer system," *IEEE Transactions on Magnetics*, vol. 55, no. 7, pp. 8001609:1-9, Jul. 2019.
- [2] Jiang, K. T. Chau, C. Liu, and C.H.T. Lee, "An overview of resonant circuits for wireless power transfer," *Energies*, vol. 10, no. 7, paper no. 894, pp. 1-20, Jun. 2017.
- [3] C. Qiu, K. T. Chau, T.W. Ching, and C. Liu, "Overview of wireless charging technologies for electric vehicles," *Journal of Asian Electric Vehicles*, vol. 12, no. 1, pp. 1679-1685, Jun. 2014.
- [4] G. A. Covic and J. T. Boys, "Inductive power transfer," *Proceedings of the IEEE*, vol. 101, no. 6, pp. 1276-1289, Jun. 2013.
- [5] W. Han, K. T. Chau, and Z. Zhang, "Flexible induction heating using magnetic resonant coupling," *IEEE Transactions on Industrial Electronics*, vol. 64, no. 3, pp. 1982-1992, Mar. 2017.
- [6] W. Han, K. T. Chau, H.C. Wong, C. Jiang, and W.H. Lam, "All-in-one induction heating using dual magnetic couplings," *Energies*, vol. 12, no. 9, paper no. 1772, pp. 1-17, May 2019.
- [7] W. Han, K. T. Chau, Z. Zhang, and C. Jiang, "Single-source multiple-coil homogeneous induction heating," *IEEE Transactions on Magnetics*, vol. 53, no. 11, pp. 7207706:1-6, Nov. 2017.
- [8] J. C. Wu, S. P. Wang, Y. H. Wang and C. Liu, "Sensitivity Analysis of Design Parameters in Transverse Flux Induction Heating Device," *IEEE Transactions on Applied Superconductivity*, vol. 30, no. 4, pp. 1-6, Jun. 2020.



- [9] C. Jiang, K. T. Chau, C. Liu, and W. Han, "Design and analysis of wireless switched reluctance motor drives," *IEEE Transactions on Industrial Electronics*, vol. 66, no. 1, pp. 245–254, Jan. 2019.
- [10] C. Jiang, K. T. Chau, T.W. Ching, C. Liu, and W. Han, "Time-division multiplexing wireless power transfer for separately excited DC motor drives," *IEEE Transactions on Magnetics*, vol. 53, no. 11, pp. 8205405:1-5, Nov. 2017.
- [11] C. Jiang, K. T. Chau, W. Liu, C. Liu, W. Han, and W.H. Lam, "An LCC compensated multiple-frequency wireless motor system," *IEEE Transactions on Industrial Informatics*, vol. 15, no. 11, pp. 6023-6034, Nov. 2019.
- [12] C. Jiang, K. T. Chau, C.H.T. Lee, W. Han, W. Liu, and W.H. Lam, "A wireless servo motor drive with bidirectional motion capability," *IEEE Transactions on Power Electronics*, vol. 34, no. 12, pp. 12001-12010, Dec. 2019.
- [13] K. H. Loo, Y. M. Lai, and C. K. Tse, "Design and analysis of LCC resonant network for quasi-lossless current balancing in multistring AC-LED array," *IEEE Transactions on Power Electronics*, vol. 28, no. 2, pp. 1047-1059, Feb. 2013.
- [14] W. Han, K. T. Chau, L. Cao, Z. Hua, and T. Yang, "S-CLC compensated wireless power transfer with pulse-frequency-modulation control for dimmable low-pressure sodium lamps," *IEEE Transactions on Magnetics*, vol. 57, no. 2, pp. 8001107:1-7, Feb. 2021.
- [15] Y. Li et al., "Analysis, design and experimental verification of a mixed high order compensations-based WPT system with constant current outputs for driving multistring LEDs," *IEEE Transactions on Industrial Electronics*, vol. 67, no. 1, pp. 203-213, Jan. 2020.
- [16] W. Han, K. T. Chau, C. Jiang, W. Liu and W. H. Lam, "Design and analysis of wireless direct-drive high-intensity discharge lamp," *IEEE Journal of Emerging and Selected Topics in Power Electronics*, vol. 8, no. 4, pp. 3558-3568, Dec. 2020.
- [17] X. Li, Y. Li, C. Tsui and W. Ki, "Wireless power transfer system with  $\Sigma\Delta$  - modulated transmission power and fast load response for implantable medical devices," *IEEE Transactions on Circuits and Systems II: Express Briefs*, vol. 64, no. 3, pp. 279-283, March 2017.
- [18] W. Han, K. T. Chau, C. Jiang and W. Liu, "Accurate position detection in wireless power transfer using magnetoresistive sensors for implant applications," *IEEE Transactions on Magnetics*, vol. 54, no. 11, pp. 1-5, Nov. 2018.
- [19] X. Tian, K. T. Chau, W. Han, and C.H.T. Lee, "Design and analysis of double-layer electromagnetic field limiter for wireless rechargeable medical implants," *IEEE Transactions on Magnetics*, vol. 57, no. 2, pp. 5100206:1-6, Feb. 2021.
- [20] O. Knecht and J. W. Kolar, "Performance evaluation of series-compensated IPT systems for transcutaneous energy transfer," *IEEE Transactions on Power Electronics*, vol. 34, no. 1, pp. 438-451, Jan. 2019.
- [21] C. C. Chan, "The state of the art of electric, hybrid, and fuel cell vehicles," *Proceedings of the IEEE*, vol. 95, no. 4, pp. 704-718, Apr. 2007.
- [22] K. T. Chau, C. Jiang, W. Han, and C.H.T. Lee, "State-of-the-art electromagnetics research in electric and hybrid vehicles," *Progress In Electromagnetics Research*, vol. 159, pp. 139-157, 2017.
- [23] C.H.T. Lee, K. T. Chau, T.W. Ching, and C.C. Chan, "Design and analysis of partitioned-stator switched-flux dual-excitation machine for hybrid electric vehicles," *World Electric Vehicle Journal*, vol. 9, no. 40, pp. 1-13, Sep. 2018.
- [24] K. T. Chau, "Energy Systems for Electric and Hybrid Vehicles," ISSN 1750-9645, *The Institution of Engineering and Technology (IET)*, 2016.
- [25] C. C. Mi, G. Buja, S. Y. Choi, and C. T. Rim, "Modern advances in wireless power transfer systems for roadway powered electric vehicles," *IEEE Transactions on Industrial Electronics*, vol. 63, no. 10, pp. 6533–6545, Oct. 2016, doi: 10.1109/TIE.2016.2574993.

- [26] C. Liu, K. T. Chau, D. Wu and S. Gao, "Opportunities and challenges of vehicle-to-home, vehicle-to-vehicle, and vehicle-to-grid technologies," *Proceedings of the IEEE*, vol. 101, no. 11, pp. 2409-2427, Nov. 2013.
- [27] S. Gao, K. T. Chau, C. Liu, D. Wu, and C.C. Chan, "Integrated energy management of plug-in electric vehicles in power grid with renewables," *IEEE Transactions on Vehicular Technology*, vol. 63, no. 7, pp. 3019-3027, Sep. 2014.
- [28] X. Dai, J. Jiang, and J. Wu, "Charging area determining and power enhancement method for multiexcitation unit configuration of wirelessly dynamic charging EV system," *IEEE Transactions on Industrial Electronics*, vol. 66, no. 5, pp. 4086-4096, May 2019.
- [29] D.-H. Kim, S. Kim, S.-W. Kim, J. Moon, I. Cho, and D. Ahn, "Coupling extraction and maximum efficiency tracking for multiple concurrent transmitters in dynamic wireless charging," *IEEE Transactions on Power Electronics*, vol. 35, no. 8, pp. 7853-7862, Aug. 2020.
- [30] C. Cai, M. Saeedifard, J. Wang, P. Zhang, J. Zhao, and Y. Hong, "A cost-effective segmented dynamic wireless charging system with stable efficiency and output power," *IEEE Transactions on Power Electronics*, vol. 37, no. 7, pp. 8682-8700, Jul. 2022.
- [31] W. Xiong, Q. Yu, Z. Liu, L. Zhao, Q. Zhu, and M. Su, "A detuning-repeater-based dynamic wireless charging system with quasi-constant output power and reduced inverter count," *IEEE Transactions on Power Electronics*, vol. 38, no. 1, pp. 1336-1347, Jan. 2023.
- [32] H. Pang, K. T. Chau, W. Liu and X. Tian, "Multi-resonating-compensation for multi-channel multi-pickup wireless power transfer," *IEEE Transactions on Magnetics*, vol. 58, no. 8, pp. 1-6, Aug. 2022, Art no. 8600506.
- [33] H. Pang, K. T. Chau, W. Han, W. Liu and Z. Zhang, "Decoupled-double D coils based dual-resonating-frequency compensation topology for wireless power transfer," *IEEE Transactions on Magnetics*, vol. 58, no. 2, pp. 1-7, Feb. 2022, Art no. 8000407.
- [34] C. Chen, Z. Wei, and A. C. Knoll, "Charging optimization for Li-ion battery in electric vehicles: A review," *IEEE Transactions on Transportation Electrification*, vol. 8, no. 3, pp. 3068-3089, Sep. 2022, doi: 10.1109/TTE.2021.3135525.
- [35] Y. Gao, X. Zhang, Q. Cheng, B. Guo, and J. Yang, "Classification and Review of the Charging Strategies for Commercial Lithium-Ion Batteries," *IEEE Access*, vol. 7, pp. 43511-43524, 2019, doi: 10.1109/ACCESS.2019.2906117.
- [36] C. Jiang, K. T. Chau, Y.Y. Leung, C. Liu, C.H.T. Lee, and W. Han, "Design and analysis of wireless ballastless fluorescent lighting," *IEEE Transactions on Industrial Electronics*, vol. 66, no. 5, pp. 4065-4074, May 2019.
- [37] C. Jiang, K. T. Chau, C. Liu, and W. Han, "Wireless DC motor drives with selectability and controllability," *Energies*, vol. 10, no. 1, paper no. 49, pp. 1-15, Jan. 2017.
- [38] C. Jiang, K. T. Chau, W. Liu, C. Liu, W. Han, and W.H. Lam, "An LCC compensated multiple-frequency wireless motor system," *IEEE Transactions on Industrial Informatics*, vol. 15, no. 11, pp. 6023-6034, Nov. 2019.
- [39] Y. Jiang, L. Wang, J. Fang, C. Zhao, K. Wang and Y. Wang, "A joint control with variable ZVS angles for dynamic efficiency optimization in wireless power transfer system," *IEEE Transactions on Power Electronics*, vol. 35, no. 10, pp. 11064-11081, Oct. 2020.
- [40] W. Liu, K. T. Chau, C. H. T. Lee, W. Han and X. Tian, "Low-frequency-switching high-frequency-resonating wireless power transfer," *IEEE Transactions on Magnetics*, vol. 57, no. 2, pp. 1-8, Feb. 2021.
- [41] W. Han, K. T. Chau, C. Jiang, W. Liu, and W.H. Lam, "High-order compensated wireless power transfer for dimmable metal halide lamps," *IEEE Transactions on Power Electronics*, vol. 35, no. 6, pp. 6269-6279, Jun. 2020.
- [42] Y. Jiang, L. Wang, Y. Wang, J. Liu, X. Li and G. Ning, "Analysis, design, and implementation of accurate ZVS angle control for ev battery charging in wireless high-power transfer," *IEEE Transactions on Industrial Electronics*, vol. 66, no. 5, pp. 4075-4085, May 2019.

- [43] W. Liu, K. T. Chau, C. H. T. Lee, C. Jiang, W. Han, and W. H. Lam, "A wireless dimmable lighting system using variable-power variable-frequency control," *IEEE Transactions on Industrial Electronics*, vol. 67, no. 10, pp. 8392-8404, Oct. 2020.
- [44] W. Liu, K. T. Chau, C.H.T. Lee, W. Han, X. Tian, and W.H. Lam, "Full-range soft-switching pulse frequency modulated wireless power transfer," *IEEE Transactions on Power Electronics*, vol. 35, no. 6, pp. 6533-6547, Jun. 2020.
- [45] W. Liu, K. T. Chau, C.H.T. Lee, X. Tian, and C. Jiang, "Hybrid frequency pacing for high-order transformed wireless power transfer," *IEEE Transactions on Power Electronics*, vol. 36, no. 1, pp. 1157-1170, Jan. 2021.
- [46] W. Liu, K. T. Chau, C.H.T. Lee, L. Cao, and C. Jiang, "Frequency-modulated wireless direct-drive motor control," *IEEE Transactions on Magnetics*, vol. 57, no. 2, Feb. 2021.
- [47] A. Namadmalan, "Self-oscillating tuning loops for series resonant inductive power transfer systems," *IEEE Trans. Power Electron.*, vol. 31, no. 10, pp. 7320-7327, Oct. 2016.
- [48] S. Assaworrorarit, X. Yu, and S. Fan, "Robust wireless power transfer using a nonlinear parity-time-symmetric circuit," *Nature*, vol. 546, no. 7658, pp. 387-390, Jun. 2017.
- [49] Z. Hua, K. T. Chau, W. Liu, and X. Tian, "Pulse frequency modulation for parity-time-symmetric wireless power transfer system," *IEEE Transactions on Magnetics*, vol. 58, no. 8, pp. 1-5, Aug. 2022.
- [50] Z. Hua, K. T. Chau, W. Liu, X. Tian and H. Pang, "Autonomous pulse frequency modulation for wireless battery charging with zero-voltage switching," *IEEE Transactions on Industrial Electronics*, Oct. 2022, early access, doi: 10.1109/TIE.2022.3215814

## Authors



**Zhichao Hua** received the B.Eng. degree in electrical engineering and automation from Wuhan University of Technology, Wuhan, China, in 2016 and the M.Eng. degree in electrical and electronic engineering from Huazhong University of Science and Technology, Wuhan, China, in 2019, respectively. He is currently working toward the Ph.D. degree in electrical and electronic engineering at the Department of Electrical and Electronic Engineering, The University of Hong Kong, Hong Kong, China. His research interests include power electronics, wireless power transfer techniques and electric vehicle technologies.



**K. T. Chau** received the B.Sc. (Eng.), M.Phil., and Ph.D. degrees in electrical and electronic engineering from The University of Hong Kong, Hong Kong, in 1988, 1991, and 1993, respectively. Since 1995, he has been with The University of Hong Kong, where he is currently a Professor in the Department of Electrical and Electronic Engineering. He is the author of nine books and more than 300 journal papers. His research interests include electric and hybrid vehicles, power electronics and drives, and renewable energies. Prof. Chau is a Fellow of the Institute of Electrical and Electronics Engineers (IEEE), U.S., the Institution of Engineering and Technology (IET), U.K., and of the Hong Kong Institution of Engineers (HKIE). He currently serves as a Coeditor of the Journal of Asian Electric Vehicles. He is a Chartered Engineer in Hong Kong. He received the Changjiang Chair Professorship from the Ministry of Education, China, and the Environmental Excellence in Transportation Award for Education, Training, and Public Awareness from the Society of Automotive Engineers (SAE) International.



**Tengbo Yang** received the B.Eng. degree in electronic information engineering from Zhejiang University, Hangzhou, China, in 2019. He is currently working toward the Ph.D. degree in electrical and electronic engineering with The University of Hong Kong, Pokfulam, Hong Kong. He received the Hong Kong Ph.D. Fellowship in 2019 to support his Ph.D. study. His research interests include electric machines and drives, electric vehicle technologies, and magnetic gears.



**Hongliang Pang** (S'17) was born in Tianjin, China. He received the B.Eng. degree in automation and M.Eng. degree in control science and engineering from Tianjin University, Tianjin, China in 2017 and 2020, respectively. He is currently working toward the Ph.D. degree in electrical and electronic engineering at the Department of Electrical and Electronic Engineering, the University of Hong Kong, Hong Kong. His current research interests include wireless power transfer and power-electronic-based impedance matching.



**Qi Zhu** received the B.S. degree in electrical engineering and automation and the Ph.D. degree in control science and engineering from Central South University, Changsha, China, in 2014 and 2019, respectively. He was a Joint Ph.D. Student from 2017 to 2019, and a Research Fellow from 2019 to 2021, both under the supervision of Prof. A. P. Hu with the University of Auckland, Auckland, New Zealand. From 2022, he is currently a Senior Hardware R&D Engineer with Xiaomi, Beijing, China. His research interests include wireless power transfer, power electronics, and renewable energy.